ACS APPLIED MATERIALS & INTERFACES

Letter

www.acsami.org

Cellulose-Nanofiber-Reinforced Poly(lactic acid) Composites Prepared by a Water-Based Approach

Tao Wang* and Lawrence T. Drzal

Composite Materials and Structures Center, Department of Chemical Engineering and Materials Science, Michigan State University (MSU), East Lansing, Michigan 48824, United States

ABSTRACT: The difficulty of dispersing cellulose nanofibers (CNFs) in hydrophobic polymers such as poly(lactic acid) (PLA) remains a major obstacle to the expansion of cellulose nanocomposite applications. In this work, we employed the solvent evaporation technique commonly used for drug microencapsulation to suspend PLA in water as microparticles. The suspension of the microparticles was easily mixed with the CNFs prepared by high-pressure homogenization. Water removal by membrane filtration produced CNF sheets filled with the particles. Compression molding of the stacked sheets resulted in nanocomposites with good CNF dispersions. Increases in the modulus and strength (up to 58% and 210%, respectively) demonstrated the load-bearing capability of the CNF network in the composites.

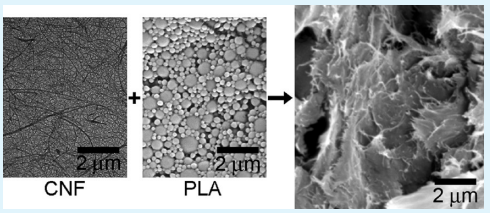

KEYWORDS: *cellulose nanofiber, poly(lactic acid), PDLLA, microparticle, nanocomposite*

INTRODUCTION

The biological nanocomposite structure of the plant cell wall gives the cells rigidity and strength as well as flexibility, which has inspired our exploration of using the main structural component of the wall, cellulose, to build biobased materials that are both useful and renewable. The basic organizational units of plant cellulose are the elementary fibrils,[1,2] which are just 3−4 nm wide and are combined to form 10−30 nm wide microfibrils.[1] The 3−4 nm structure is often also named directly as a microfibril, and the thicker structures are then called microfibril aggregates or composite fibers.[3,4] The most popular mechanical process to disintegrate the natural cellulose microfibril assembly is through high-pressure homogenization of a cellulose−water suspension.[5,6] The product, named microfibrillated cellulose (MFC), consists of fibers that can have a wide width distribution depending on the degree of fibrillation. With multiple passes at high pressures or with surface modifications, MFC can be produced with average widths well below 100 nm and is increasingly referred to as cellulose nanofiber, nanofibril, nanofibrillated cellulose, and nanocellulose.[2] The authors choose the term cellulose nanofiber (CNF) to avoid contrasting words like nanofibril and nanofibrillated with the microfibril (a biological structure) and microfibrillated terminology, where "micro" simply means small. "Nanocellulose" is used as a broad term to include CNF, cellulose nanowhisker (CNW), and bacterial cellulose. The order of packing of elementary fibrils within a microfibril is very high, as predicted in cellulose ultrastructure models.[7] The lowest width of CNFs produced by mechanical disintegration of natural cellulose is usually above 10 nm.[8] Thinner CNFs are obtained after surface modifications such as TEMPO-mediated oxidation.[9] The acid hydrolysis used for CNW production also results in lower width.[10] These products can have a width of 3−5 nm, corresponding to the width of elementary fibrils.

Although the high stiffness, aspect ratio, and relative surface area of nanocellulose make it an attractive reinforcing material for biopolymers in medical and structural applications, industrially feasible methods to produce cellulose nanocomposites are lacking. The highly hydrophilic surface of cellulose makes it difficult to prevent fiber aggregation in hydrophobic polymers such as poly(lactic acid) (PLA). Satisfactory nanocellulose dispersion is often achieved only in thin films. Various processing strategies have significant challenges to be overcome to address this issue. For example, feeding cellulose suspensions directly into the polymer melt in an extruder results in fiber agglomeration.[11] Adding nanocellulose into the solution or suspension of monomers or prepolymers enables easy mixing before in situ polymerization or cure.[12−14] However, in several studies, cellulose and water have been found to interfere with the polymerization reactions and to introduce defects in the composites.[15,16] Waterborne polymers are mainly used as adhesives and coatings. In another approach, cellulose suspensions are filtered to yield thin films, which can be embedded in and cured with thermosetting resins[17] or be sandwiched between polymer sheets and hot-pressed into laminates.[18−20] The cellulose films are sometimes surface-treated to prevent delamination.[20] The densely packed nanocellulose network makes polymer penetration difficult. Alternatively, polymer latex or fibers are mixed with MFC suspensions directly and are filtered to produce films or sheets that can be melt-processed.[21−23]

When a solvent is used, nanocellulose is transferred from water to the solvent by direct mixing (for a water-miscible solvent),[24] by solvent exchange,[25,26] or by drying and

Received: July 24, 2012
Accepted: September 13, 2012
Published: September 19, 2012

 © 2012 American Chemical Society dx.doi.org/10.1021/am301438g | ACS Appl. Mater. Interfaces 2012, 4, 5079−5085

redispersion[25−27] and is then mixed with the polymer solution. Solvent exchange and freeze-drying are both laborious and expensive procedures. Dispersing natural cellulose in low-polarity organic solvents is usually difficult. This method is mainly used to cast thin films or to produce electrospun fiber mats.

Surface treatments such as coating with surfactants,[28] controlled oxidation (e.g., TEMPO-mediated oxidation),[29] and functionalizations (e.g., silylation,[30] carboxymethylation,[31] isocyanate grafting,[32] and esterification with organic acids[33,34]) have been used to prevent the irreversible agglomeration of nanocellulose upon drying and to facilitate its dispersion in organic solvents and hydrophobic polymers. Polymer grafting is particularly useful for enhancing interfacial adhesion.[35] The large surface area of nanocellulose with a high density of hydroxyl groups on it requires a high loading of chemicals for coating.[36] More importantly, the reinforcing effect of cellulose in polymer composites has been attributed not only to its high stiffness but also to its tendency of forming percolating networks through hydrogen bonding. When nanocellulose is modified to be less likely to aggregate as a result of weakened interfibrillar affinity, its ability to cross-link into strong networks may be sacrificed too,[37,38] which may explain some observations of little or no property enhancement after the modifications despite improved dispersions.[33,39,40]

The present work is aimed at contributing to the effort of finding an effective and practical way to produce cellulose nanocomposites with a process that begins with dispersion of the polymer in water. The solvent evaporation technique used in the pharmaceutical industry for drug microencapsulation was adapted here to make PLA microparticles. The mixture of the particles and CNF was filtered and dried into CNF sheets filled with the particles. Composites (1.4 mm in thickness) were prepared from the sheets and were then characterized for their microstructures and mechanical and thermal properties.

EXPERIMENTAL SECTION

Materials. The raw material for CNF production was CreaTech TC90 cellulose fibers provided by CreaFill Fibers Corp. (Chestertown, MD). The product is in dry powder form and contains 99.5% α-cellulose extracted from wood. The average width and length of the fibers are 20 and 60 μm, respectively. PLA used was PURASORB PDL 04, a poly(DL-lactide) (PDLLA) product purchased from PURAC America, Inc. (Lincolnshire, IL). Its inherent viscosity midpoint was 0.39 dL/g (tested at 1.0 g/dL in chloroform), corresponding to a weight-average molecular weight of ~45000 g/mol. Polysorbate 80 (aka TWEEN 80) and ethyl acetate were purchased from Sigma-Aldrich Co. (St. Louis, MO) and EMD Chemicals Inc. (Gibbstown, NJ), respectively, and were used as received.

CNF Preparation. The wood cellulose fibers were dispersed in water at 0.4 wt % with a kitchen blender. CNF was then obtained by homogenizing the suspension with a 0.008 in. (0.20 mm) nozzle at 16000 psi (110 MPa) for 4 passes and with a 0.005 in. (0.13 mm) nozzle at about 42000 psi (290 MPa) for 20 passes, using a Mini DeBEE ultrahigh-pressure homogenizer (BEE International, South Easton, MA). The flow pattern was single-jet parallel flow with zero backpressure. A total of 11 "reactors" (zirconium cylinders with 1.0-mm-diameter orifice) were installed after the nozzle in the emulsifying cell. The suspension was water-cooled with a heat exchanger after each pass through the homogenizer. There was some sample loss due to material holdup in the hoses and fittings of the machine. The weight contents of the final suspensions were tested to be in the range of 0.30−0.33%. Transmission electron microscopy (TEM) specimens were prepared by ultrasonication of a diluted suspension for about 30 s with a VirTis VirSonic-100 cell disrupter (SP Industries Inc., Warminster, PA) and drying of a tiny drop on a Formvar-coated carbon grid. Observations were made using a JEOL 100CX transmission electron microscope operated at 100 kV.

PDLLA Microparticles. Polysorbate 80 (0.12 g) was dissolved in 160 mL of water by agitation with an IKA Ultra-Turrax T 25 homogenizer equipped with a S25N-25F dispersing element at 8000 rpm for 5 min (IKA Works Inc., Wilmington, NC). PDLLA granules (4.00 g) were dissolved in 40 mL of ethyl acetate before being emulsified into the Polysorbate water solution by using the Ultra-Turrax homogenizer running at 10000 rpm for 10 min. The emulsion was ultrasonicated with a 1-in. probe installed on a Cole-Parmer ultrasonic processor (Vernon Hills, IL) at 100 W for 2 min to further reduce the droplet size. The evaporation of ethyl acetate was carried out in a 40 °C water bath overnight, resulting in a milky suspension of PDLLA microparticles. A few drops of the suspension was filtered with a 0.1 μm pore size mixed-cellulose-ester membrane filter (Advantec MFS Inc., Dublin, CA). The membrane, carrying a small amount of the particles, was then gold-coated by sputtering and imaged with a JEOL JSM-6400 scanning electron microscope at an accelerating voltage of 10 kV. The suspensions were tested for their weight contents and typically contained 3.8 g of solids in each batch.

Nanocomposite Fabrication. An appropriate amount of the CNF suspension was added to the PDLLA suspension, stirred for 1 h, and immediately vacuum filtered using Millipore Durapore PVDF membrane filters with 90 mm in diameter and 0.65 μm in pore size (Fisher Scientific, Pittsburgh, PA). The paste collected on the filter membrane was air-dried for 2−3 days. The dried sample cake was found to have a two-layered structure consisting of a self-standing PDLLA-filled CNF sheet on top of a loosely bonded layer of precipitated microparticles. The bottom layer of the microparticles would crumble into fine powder when pressed by hand and could be dissolved into ethyl acetate as a clear solution, showing no sign of CNF presence. The PDLLA-CNF sheets were removed from the cakes and were compression-molded using stainless-steel picture-frame molds (1.4 mm thick) on a Carver Laboratory Press (Carver Inc., Wabash, IN) at 105 °C and 90 psi (0.6 MPa). Three composites were prepared. Their actual weight contents were calculated to be 8, 15, and 32% by dividing the dry weight of the loaded CNF by the weight of the molded composites. The 8 and 15 wt % samples were prepared by molding six and five layers of sheets stacked together. Because a higher CNF content led to a higher amount of microparticles retained in the cellulose gel formed during the filtration and, in turn, a thicker PDLLA-CNF sheet obtained, the 32 wt % composite was molded from just one sheet. A control sample was made by filtering a PDLLA suspension and compression molding using the same procedure.

Composite Characterization. Flexural properties were measured using a universal testing machine (United Calibration Corp. model SFM-20, Huntington Beach, CA). Rectangular specimens (38.1 × 12.7 × 1.40 mm^3) were cut out from the composites, conditioned in 50% relative humidity at room temperature for about 40 h, and tested to failure at a span distance of 1.00 in. (25.4 mm) and a crosshead speed of 0.03 in.

(0.76 mm) per 1 min. Three to four tests were conducted for each sample. The fracture surfaces created by flexural testing were gold-coated by sputtering and imaged with the JEOL JSM-6400 operated at 10 kV. Dynamic mechanical analysis (DMA) was performed in three-point bending mode using a TA Instruments Q800 analyzer (New Castle, DE). Test specimens were 8−12 mm wide and ∼35 mm long and were conditioned in the same manner as above. The support span, frequency, and amplitude of oscillation were set at 20 mm, 1 Hz, and 70 μm, respectively. The specimens were tested in air at a heating rate of 3 °C/min, from 25 °C until they had failed or the measured modulus had reached a plateau. The as-received PDLLA and the molded samples were analyzed by differential scanning calorimetry (DSC) using a TA Instruments Q2000 analyzer. Under nitrogen purge, the samples (7−8 mg) contained in aluminum pans were heated from 5 to 105 °C, held at 105 °C for 5 min, cooled to 5 °C, and heated again to 105 °C. Both the heating and cooling rates were 10 °C/min.

RESULTS AND DISCUSSION

The high shear force generated by the homogenizer breaks down the fibrillar structure of the cellulose fibers to release their constituent microfibrils into water to form a stable suspension. TEM observation showed that, although the fiber width distribution was not uniform, the dominant morphology was nanofibers with widths on the order of 20−30 nm (Figure 1). These widths agree with the 18 nm diameter measured for wood cellulose microfibrils[41] and are thicker than the width of elementary fibrils.[1]

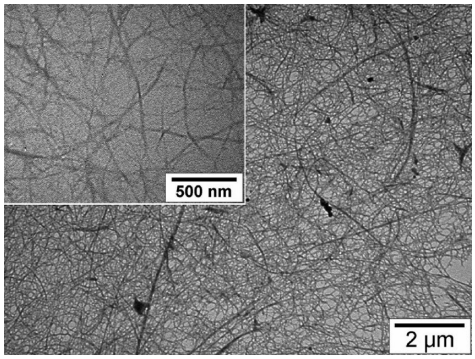

Figure 1. TEM micrographs of CNFs prepared from wood cellulose.

Because lactic acid is a chiral molecule, three different forms of PLA, namely, PLLA, PDLA, and PDLLA, exist. Adding nanofillers to semicrystalline polymers such as PLLA and PDLA may change their crystallization behavior, leading to mechanical property changes. We chose the amorphous PDLLA in this work to eliminate the nucleation factor from the analysis. In the solvent evaporation technique, PLA is first dissolved in a volatile organic solvent to form the oil phase, which is then emulsified with a high-speed mixer into a continuous water phase as discrete oil droplets. A suitable surfactant is used to stabilize the emulsion. The organic solvent is then evaporated from the emulsion under stirring to let the oil droplets harden to form microparticles.[42,43] The diameters of the particles obtained varied widely, ranging from about 150 nm to more than 1 μm (Figure 2). A nonuniform particle size distribution is common in drug microencapsulation using this technique.[42] Although polymer particles with near-uniform sizes below 200 nm can be produced, an excess amount of

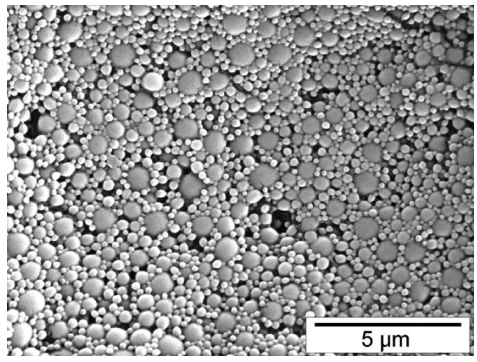

Figure 2. SEM micrograph of PDLLA microparticles produced by solvent evaporation.

surfactant (50−100% of the polymer weight) is usually required.[44,45] In addition, the most popular stabilizer used for PLA emulsification in the pharmaceutical industry, poly(vinyl alcohol),[46] is immiscible with PLA when melt-processed.[47] After screening various surfactants (data not shown), we found that Polysorbate 80 (an ester of polyethoxylated sorbitan and oleic acid) was effective in stabilizing these emulsions at a very low surfactant-to-polymer weight ratio of 3:100. Using a minimal amount of surfactant avoids property changes induced by the residual chemical.

Because water keeps the CNF and polymer dispersed in their mixture, cellulose agglomeration and particle sedimentation can happen during water removal. In one experiment, the mixture was quickly frozen in liquid nitrogen and freeze-dried into a fine powder. After compression molding, large aggregates of CNFs were found in the clear PDLLA matrix (data not shown). When water is frozen into ice, the spontaneous nucleation of ice crystals drives the dissolved or suspended substances out, concentrating them in the shrinking water phase. This caused the cellulose to agglomerate even before the sublimation process took place. Water removal by membrane filtration was found to be like a sol−gel process except that the gelation was not caused by chemical cross-linking but by the concentrated CNFs. Before filtration, the mixture was a free-flowing liquid sol of suspended CNFs and microparticles. With water being drawn away by vacuum, the mixture became a gel-like material when the CNFs were concentrated to form a continuous network, trapping the microparticles. Only a fraction of all of the particles in the mixture (from 34 to 63%) could be retained by the gel, while the rest precipitated out from the network, resulting in a two-layered wet cake formed on the membrane. The phenomenon could have been caused by the difference in the stabilities of CNF and PDLLA in water and the nonuniform size distribution of the microparticles. Reducing particle sizes with higher surfactant loadings and increasing the filtration speed (to about 15 s per batch) by feeding smaller sample volumes or by using large-pore-size membrane filters did not prevent it from happening (data not shown). Nevertheless, after drying, the upper layers of the sample cakes became CNF sheets filled with the polymer particles and were compression-molded into CNF/PDLLA composites. The neat PDLLA control sample is transparent, and the 8, 15, and 32 wt % composites are opaque with an off-white color. Nanocellulose (often more uniform bacterial cellulose) has been impregnated with transparent resins to prepare transparent thin films.[8] Although the PDLLA-CNF sheets were prepared by filtration, the presence of microparticles did not allow the fibers to be

arranged in the same way as that in a CNF film. Also, because of the nonuniform width distribution of the CNFs and the fact that they were entangled in 1.4-mm-thick molded sheets, optical transparency was not expected for these composites.

Both the flexural modulus and strength (stress at break) of the composites grew progressively with increasing CNF content (Figure 3). At 32 wt % CNF loading, the modulus and strength

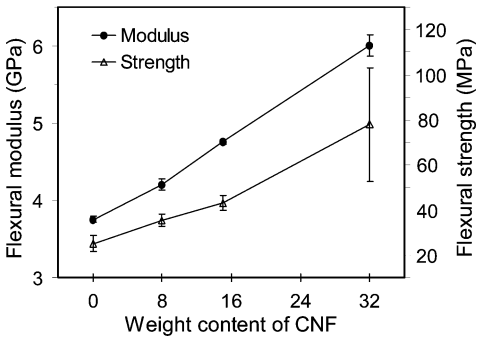

Figure 3. Flexural modulus and strength of the neat PDLLA and the 8, 15, and 32 wt % CNF/PDLLA composites.

of PDLLA were improved 58% (from 3.8 to 6.0 GPa) and 210% (from 25 to 78 MPa), respectively. The high aspect ratio of the CNFs and their strong web structures contributed greatly to the large strength improvement. A similar filtration process has been used by Nakagaito et al. and Larsson et al. to fabricate cellulose nanocomposites using commercially available PLA fiber and latex, respectively.[22,23] The composite sheets (300 μm thick) and films obtained by hot-pressing are tested for their tensile properties. Thicker samples prepared in the present work enabled us to conduct three-point bending test, eliminating the need for gripping the brittle PLA for the tensile test. The linear increase in the flexural properties measured agrees with the tensile property improvements observed by the above two groups at the same range of CNF loadings. Figure 4 shows that the strain at break of PDLLA was

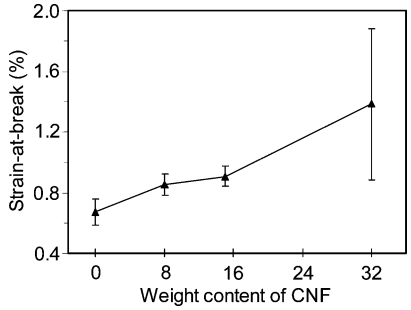

Figure 4. Comparison of the strain at break of the neat PDLLA and the CNF/PDLLA composites.

also increased by the addition of the CNFs. This is a good indication of fiber dispersion because the agglomeration of cellulose in PLA often leads to strain decreases.[34,48] On the other hand, the strain-at-break values of the three composites were not significantly different, which is also found in Nakagaito et al. and Larsson et al.'s experiments, where a further increase of the strain at break is only achieved at above 40% fiber loadings. At high CNF content, the CNF paper has probably started to control the composite properties. Reinforcement with nanocellulose seems to have only a limited ability to enhance the toughness of PLA unless the adhesion between the fiber and matrix can be improved.

The storage modulus (E') of the composites was also higher than that of the neat polymer throughout the temperature range tested (Figure 5a). A linear increase with the CNF

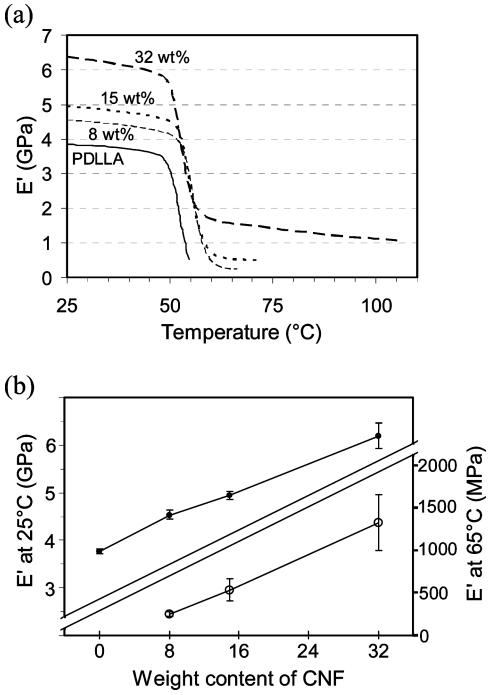

Figure 5. (a) Storage moduli of the neat PDLLA and the CNF/PDLLA composites as a function of the temperature. Testing of the neat PDLLA was stopped when it softened to yield under the applied load. Testing of the 8 and 15 wt % composites was stopped when the specimens fractured. The 32 wt % composite was tested to 105 °C. (b) Comparison of the storage moduli at 25 and 65 °C (no value was measured for the neat PDLLA at 65 °C).

content was found both before and after glass transition (Figure 5b). At 25 °C, the storage modulus of 32 wt % CNF/PDLLA was 6.2 GPa, compared to 3.8 GPa of the neat polymer (a 63% increase). When amorphous PDLLA turned from a brittle glassy material into a soft material above its T_g, losing its stiffness quickly, the structural integrity of the composites was still maintained by the CNFs. The modulus of 32 wt % CNF/PDLLA did not drop below 1 GPa even when the temperature rose 50 °C above its T_g. The 8 and 15 wt % composites also remained brittle and did not yield but fractured at the end of testing. This shows clearly that the CNF has formed a load-bearing network in the polymer matrix and is acting more as a continuous phase than just as conventional fillers, which probably would have flowed with the polymer. The same behavior has also been observed after the melting of the semicrystalline PLA in the cellulose nanocomposites prepared by Nakagaito et al. and Larsson et al., at 70 wt % and higher and 25 wt % and higher cellulose contents, respectively.[22,23]

The effect of CNF reinforcement on the glass transition of polymers is more complex. Mixed results have been reported regarding the T_g shift in cellulose nanocomposites.[23,28,49] Factors contributing to the T_g increase include the stiffness of nanocellulose and increased crystallinity. The plasticizing effect of the adsorbed water and the compatibilizers and surfactants added can lead to a T_g decrease. In this work, the onset of the

dx.doi.org/10.1021/am301438g | ACS Appl. Mater. Interfaces 2012, 4, 5079−5085

E' drop of the 8 and 15 wt % composites was about 3 °C higher than that of the neat PDLLA, while the onset of the E' drop of the 32 wt % composite was the same as that of the neat polymer (see Figure 5a). The same trend can also be seen in the evolution of the tan δ peaks (Figure 6). The quick softening

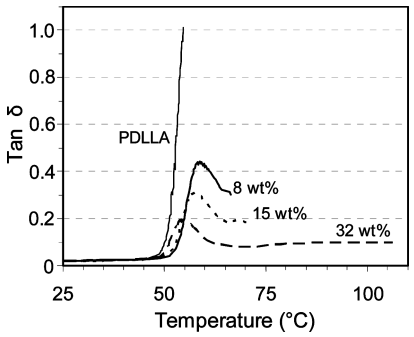

Figure 6. tan δ of the neat PDLLA and the CNF/PDLLA composites as a function of the temperature.

of the neat PDLLA did not allow a tan δ peak to be recorded. However, the failure of the material itself and the tan δ value of 1.0 suggests that the location of the maximum would be near the peak if such a peak had existed. The decreasing height of the tan δ peaks with increasing CNF content was expected because the amorphous polymer's content and contribution to the overall material property was decreasing. Compared to the location of the tan δ maximum of the neat polymer, the temperatures of the tan δ peaks of the 8 and 15 wt % composites were about 4 and 3 °C, respectively, higher, while the tan δ peak of the 32 wt % composite was at the same temperature. The T_g of the materials was also studied with DSC. For amorphous polymers with T_g not far from room temperature, physical aging can occur and its relaxation can be observed as an endothermic peak just above T_g on the DSC curve. During the first heating scan, the as-received PDLLA and the processed samples all showed large and sharp stress relaxation peaks (Figure 7). From Figure 7 and Table 1, it can be seen that the onset of the stress relaxation was delayed about 3 °C for the 8 wt % composite compared to the neat polymer (control) and the 32 wt % composite. This is the same trend as that observed for the evolution of the tan δ peaks. During the second heating scan, a typical stepwise change in the heat flow

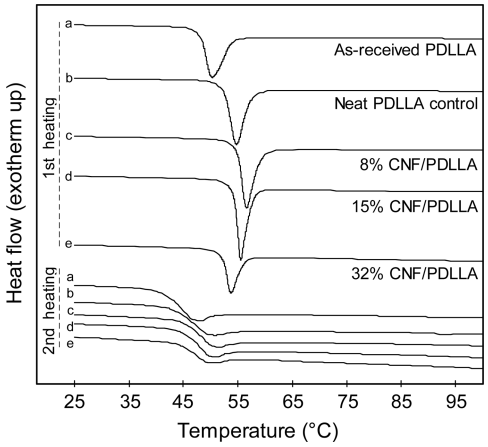

Figure 7. DSC traces obtained during the first and second heating scans.

Table 1. DSC Analysis of PDLLA and CNF/PDLLA Composites (Heating/Cooling/Heating between 5 and 105 °C)

material	onset of stress relaxation during the first heating (°C)	T_g measured during the second heating (°C)
as-received PDLLA	48.1	43.3
PDLLA (control)	52.0	45.7
8% CNF/PDLLA	54.9	47.0
15% CNF/PDLLA	54.2	46.5
32% CNF/PDLLA	52.2	46.0

was obtained and T_g determined by the midpoint of the change became almost the same for the neat polymer and the composites (46–47 °C). On the basis of the DMA and DSC analysis, we speculate that the rigid CNF network may have hindered the segmental movement of PDLLA chains, while the bound water of cellulose may have had a plasticizing effect on the polymer because the chain end groups of PLA are polar. The combined effect caused T_g to increase slightly at lower CNF content and fall back at increased CNF content. The lack of chemical interaction was then reflected by the same T_g as that observed for the polymer and the composites during the second heating run.

While a clean and smooth fracture is typical for a brittle material like PDLLA after flexural testing, the composites had very rough fracture surfaces (Figure 8). The ends of the CNFs prodtruding from the polymer matrix gave these surfaces a hairy appearance. This hairy morphology was found throughout the surfaces, indicating good dispersions (Figure 8b,d,f). On the

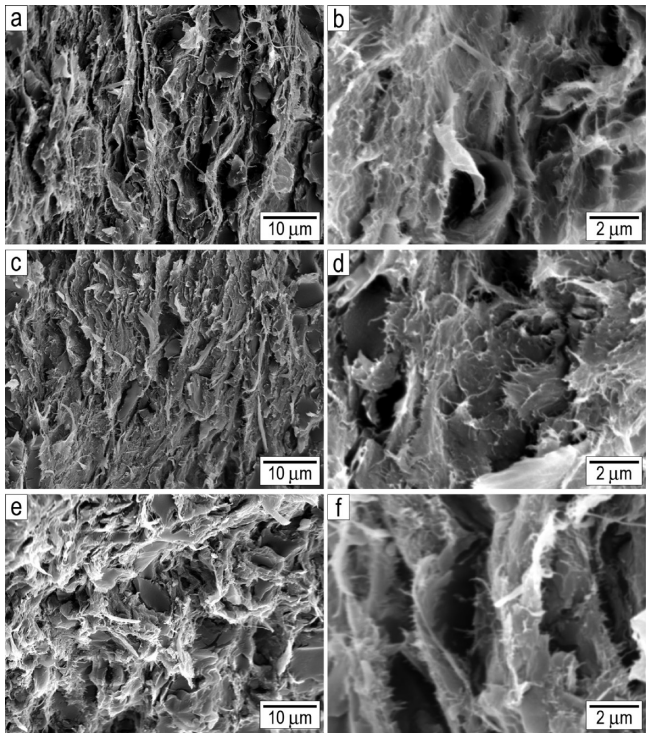

Figure 8. Fracture surfaces of the 8 (a and b), 15 (c and d), and 32 (e and f) wt % CNF/PDLLA composites. No laminated structures are present. CNF pull-outs as well as voids and cracks can be seen.

dx.doi.org/10.1021/am301438g | ACS Appl. Mater. Interfaces 2012, 4, 5079–5085

other hand, the appearance of a large number of CNFs pulled out from the surfaces by mechanical testing also suggests weak adhesion. No laminated structures commonly found in nanocomposites prepared by filtration were present. The use of a picture-frame mold with a fixed thickness may have resulted in the material not experiencing enough pressure when molded, leaving voids in the samples. The low compatibility of cellulose and PLA could also contribute to the presence of voids and cracks. The load applied during flexural testing may have caused some of the cracks to grow, pulling out fibers on both sides of the cracks (Figure 8f). The number of cracks resulting from interfacial debonding and voids were higher in the 32 wt % composite than in the 8 and 15 wt % samples, which may explain the large deviation in the strength and strain at break measured for the 32 wt % composite in Figures 3 and 4.

The solvent evaporation technique is simple and inexpensive. Both the water and solvent can be recycled. This approach can be used with different polymers and offers a great deal of freedom in tuning the size and surface chemistry of the particles. The weak interaction between the polymer and cellulose in a mixture ultimately limits the choice of drying methods and the overall process efficiency. It has been shown that the electrostatic force can be used to adhere negatively charged CNWs onto positively charged poly(butyl methacrylate) particles synthesized by in situ emulsion polymerization and to adsorb self-assembled cationic block copolymer micelles onto anionic carboxymethylated CNFs.[14,50] If similar techniques can be employed to enhance the affinity between CNF and polymer in a mixture, industrial-scale dryers can then be used for water removal without causing cellulose agglomeration. The solids thus produced can be easily stored, transported, and melt-processed into various articles.

CONCLUSIONS

A fabrication process free of toxic organic solvents was developed to achieve homogeneous distribution of CNF in polymer nanocomposites. By preparing PDLLA microparticles with a simple solvent evaporation technique, using a small amount of Polysorbate 80 as the surfactant, we were able to disperse the polymer in water for mixing with the CNFs. The mixture was filtered and dried to yield particle-filled CNF sheets. Compression molding of the sheets melted the microparticles to effectively incorporate the CNF in the composites. With good dispersions achieved, the CNFs improved both the stiffness and strength of the polymer. The stiffness of the CNF network itself became more evident after the amorphous polymer transitioned into the viscous region above its T_g. At present, not all of the particles in the mixture are retained by the CNF sheets after filtration. Higher suspension stability and stronger fiber−polymer interaction will be required to improve this method. Because both pure cellulose and Polysorbate 80 are biocompatible, these nanocomposites are potentially useful for expanding PLA applications in tissue engineering and orthopedic surgery.

AUTHOR INFORMATION

Corresponding Author

*E-mail: wangtao@msu.edu.

Notes

The authors declare no competing financial interest.

ACKNOWLEDGMENTS

Funding support from MBI International (Lansing, MI) is gratefully acknowledged. The authors thank Alicia Pastor, Ewa Danielewicz, Carol Flegler, and Xudong Fan in the Center for Advanced Microscopy at MSU for their assistance with electron microscopic imaging. T.W. is indebted to Drs. Jue Lu, Wanjun Liu, Hiroyuki Fukushima, and Toshiya Kamae for their generous assistance and advice.

REFERENCES

(1) O'Sullivan, A. C. *Cellulose* **1997**, *4*, 173−207.
(2) Chinga-Carrasco, G. *Nanoscale Res. Lett.* **2011**, *6*, 417.
(3) Ohad, I.; Mejzler, D. *J. Polym. Sci., Part A: Gen. Pap.* **1965**, *3*, 399−406.
(4) Hult, E.-L.; Iversen, T.; Sugiyama, J. *Cellulose* **2003**, *10*, 103−110.
(5) Turbak, A. F.; Snyder, F. W.; Sandberg, K. R. *J. Appl. Polym. Sci.: Appl. Polym. Symp.* **1983**, *37*, 815−827.
(6) Herrick, F. W.; Casebier, R. L.; Hamilton, J. K.; Sandberg, K. R. *J. Appl. Polym. Sci.: Appl. Polym. Symp.* **1983**, *37*, 797−813.
(7) Mühlethaler, K. *Annu. Rev. Plant Physiol.* **1967**, *18*, 1−24.
(8) Siró, I.; Plackett, D. *Cellulose* **2010**, *17*, 459−494.
(9) Isogai, A.; Saito, T.; Fukuzumi, H. *Nanoscale* **2011**, *3*, 71−85.
(10) Fleming, K.; Gray, D. G.; Matthews, S. *Chem. Eur. J.* **2001**, *7*, 1831−1835.
(11) Mathew, A. P.; Chakraborty, A.; Oksman, K.; Sain, M. In *Cellulose Nanocomposites: Processing, Characterization, and Properties*; Oksman, K., Sain, M., Eds.; American Chemical Society: Washington DC, 2006; p 114.
(12) Cao, X.; Dong, H.; Li, C. M. *Biomacromolecules* **2007**, *8*, 899−904.
(13) Liu, H.; Laborie, M.-P. G. *Cellulose* **2011**, *18*, 619−630.
(14) Mabrouk, A. B.; Vilar, M. R.; Magnin, A.; Belgacem, M. N.; Boufi, S. *J. Colloid Interface Sci.* **2011**, *363*, 129−136.
(15) Funabashi, M.; Kunioka, M. *Macromol. Symp.* **2005**, *224*, 309−321.
(16) Duanmu, J.; Gamstedt, E. K.; Rosling, A. *J. Compos. Mater.* **2012**, DOI: 10.1177/0021998312437000.
(17) Masoodi, R.; El-Hajjar, R. F.; Pillai, K. M.; Sabo, R. *Mater. Des.* **2012**, *36*, 570−576.
(18) Quero, F.; Nogi, M.; Yano, H.; Abdulsalami, K.; Holmes, S. M.; Sakakini, B. H.; Eichhorn, S. J. *ACS Appl. Mater. Interfaces* **2010**, *2*, 321−330.
(19) Cherian, B. M.; Leão, A. L.; de Souza, S. F.; Costa, L. M. M.; de Olyveira, G. M.; Kottaisamy, M.; Nagarajan, E. R.; Thomas, S. *Carbohydr. Polym.* **2011**, *86*, 1790−1798.
(20) Panthapulakkal, S.; Sain, M. *Int. J. Polym. Sci.* **2012**, 1−6.
(21) Okubo, K.; Fujii, T.; Yamashita, N. *JSME Int. J., Ser. A* **2005**, *48*, 199−204.
(22) Nakagaito, A. N.; Fujimura, A.; Sakai, T.; Hama, Y.; Yano, H. *Compos. Sci. Technol.* **2009**, *69*, 1293−1297.
(23) Larsson, K.; Berglund, L. A.; Ankerfors, M.; Lindström, T. *J. Appl. Polym. Sci.* **2012**, *125*, 2460−2466.
(24) Schroers, M.; Kokil, A.; Weder, C. *J. Appl. Polym. Sci.* **2004**, *93*, 2883−2888.
(25) Tang, L.; Weder, C. *ACS Appl. Mater. Interfaces* **2010**, *2*, 1073−1080.
(26) Sanchez-Garcia, M. D.; Lagaron, J. M. *Cellulose* **2010**, *17*, 987−1004.
(27) Ten, E.; Turtle, J.; Bahr, D.; Jiang, L.; Wolcott, M. *Polymer* **2010**, *51*, 2652−2660.
(28) Fortunati, E.; Armentano, I.; Zhou, Q.; Iannoni, A.; Saino, E.; Visai, L.; Berglund, L. A.; Kenny, J. M. *Carbohydr. Polym.* **2012**, *87*, 1596−1605.
(29) Johnson, R. K.; Zink-Sharp, A.; Renneckar, S. H.; Glasser, W. G. *Cellulose* **2009**, *16*, 227−238.
(30) Raquez, J.-M.; Murena, Y.; Goffin, A.-L.; Habibi, Y.; Ruelle, B.; DeBuyl, F.; Dubois, P. *Compos. Sci. Technol.* **2012**, *72*, 544−549.

(31) Eyholzer, Ch.; Lopez-Suevos, F.; Tingaut, P.; Zimmermann, T.; Oksman, K. *Cellulose* **2010**, *17*, 793−802.
(32) Siqueira, G.; Bras, J.; Dufresne, A. *Biomacromolecules* **2009**, *10*, 425−432.
(33) de Menezes, A. J.; Siqueira, G.; Curvelo, A. A. S.; Dufresne, A. *Polymer* **2009**, *50*, 4552−4563.
(34) Tomé, L. C.; Pinto, R. J. B.; Trovatti, E.; Freire, C. S. R.; Silvestre, A. J. D.; Neto, C. P.; Gandini, A. *Green Chem.* **2011**, *13*, 419−427.
(35) Lönnberg, H.; Larsson, K.; Lindström, T.; Hult, A.; Malmström, E. *ACS Appl. Mater. Interfaces* **2011**, *3*, 1426−1433.
(36) Heux, L.; Chauve, G.; Bonini, C. *Langmuir* **2000**, *16*, 8210−8212.
(37) Lee, K.-Y.; Quero, F.; Blaker, J. J.; Hill, C. A. S.; Eichhorn, S. J.; Bismarck, A. *Cellulose* **2011**, *18*, 595−605.
(38) Goffin, A.-L.; Raquez, J.-M.; Duquesne, E.; Siqueira, G.; Habibi, Y.; Dufresne, A.; Dubois, P. *Biomacromolecules* **2011**, *12*, 2456−2465.
(39) Tingaut, P.; Zimmermann, T.; Lopez-Suevos, F. *Biomacromolecules* **2010**, *11*, 454−464.
(40) Veigel, S.; Müller, U.; Keckes, J.; Obersriebnig, M.; Gindl-Altmutter, W. *Cellulose* **2011**, *18*, 1227−1237.
(41) Fahlén, J.; Salmén, L. *J. Mater. Sci.* **2003**, *38*, 119−126.
(42) O'Donnell, P. B.; McGinity, J. W. *Adv. Drug Delivery Rev.* **1997**, *28*, 25−42.
(43) Mathiowitz, E.; Kreitz, M. R.; Brannon-Peppas, L. In *Encyclopedia of Controlled Drug Delivery*; Mathiowitz, E., Ed.; John Wiley & Sons: New York, 1999; Vol. 2, p 504.
(44) Barichello, J. M.; Morishita, M.; Takayama, K.; Nagai, T. *Drug Dev. Ind. Pharm.* **1999**, *25*, 471−476.
(45) Ravi Kumar, M. N. V.; Bakowsky, U.; Lehr, C. M. *Biomaterials* **2004**, *25*, 1771−1777.
(46) Vandervoort, J.; Ludwig, A. *Int. J. Pharm.* **2002**, *238*, 77−92.
(47) Shuai, X.; He, Y.; Asakawa, N.; Inoue, Y. *J. Appl. Polym. Sci.* **2001**, *81*, 762−772.
(48) Jonoobi, M.; Harun, J.; Mathew, A. P.; Oksman, K. *Compos. Sci. Technol.* **2010**, *70*, 1742−1747.
(49) Lu, J.; Wang, T.; Drzal, L. T. *Composites, Part A* **2008**, *39*, 738−746.
(50) Wang, M.; Olszewska, A.; Walther, A.; Malho, J.-M.; Schacher, F. H; Ruokolainen, J.; Ankerfors, M.; Laine, J.; Berglund, L. A.; Osterberg, M.; Ikkala, O. *Biomacromolecules* **2011**, *12*, 2074−2081.